

## High Resolution Scanning Configurations for the Canberra Tomographic Gamma Scanner – 17323

J. M. Kirkpatrick\*, D. Nakazawa\*, S. K. Smith\*, \*\*, P. McClay\*,  
D. Petroka\*, M. Villani\*, X. Ducoux\*, S. Philips\*

\*Canberra Industries, Inc.

\*\*Oak Ridge National Laboratory

### ABSTRACT

The Canberra Tomographic Gamma Scanner (TGS) is a Non-Destructive Assay (NDA) system that combines high resolution gamma ray spectroscopy (HRGS) with low-spatial-resolution imaging for the measurement of heterogeneous drummed waste with matrix densities in the range of 0 to 1 g/cc. The TGS methodology uses a two-pass scanning protocol; a 10-15  $\mu\text{Ci}$   $^{152}\text{Eu}$  transmission source is used to interrogate density and composition of the matrix in the first pass, and passive gamma ray spectroscopy is used to collect emission spectra in the second, while the drum is rotated and translated to vary the view path. In standard implementations, the transmission and emission data are used to reconstruct three dimensional images of the matrix and activity distribution inside the drum on a  $10 \times 10 \times 16$  grid of discrete volume elements or "voxels". These images allow attenuation corrections to be calculated and applied on a view by view, and voxel by voxel basis, reducing the over- and under-correction biases obtained by assay techniques which assume homogeneous distributions of material. The most recent TGS system deployed by Canberra featured, among other new developments, the ability to perform higher resolution image reconstruction, which may prove beneficial for the assay of more highly mixed matrices or oddly shaped assay items within a container. These additional scanning protocols reconstruct the image data into  $14 \times 14$  and  $20 \times 20$  voxel grids, using a smaller collimator aperture size. The hardware and software implementations of these higher resolution scans are discussed, and the calibration and initial evaluations of performance are presented

### INTRODUCTION

TGS systems have been commercially employed in assaying radioactive waste generated by nuclear power plants as well as facilities handling special nuclear materials (SNM). The default scanning resolution and settings originally proposed by the LANL developers of the TGS algorithms was intended for 200L drums and some basic assumptions on drum contents (sample) and performance. While these settings have proven to be appropriate for most measurement situations, it is reasonable to raise the following questions: (i) Are the default settings applicable to smaller (or different) sized containers; (ii) Are they appropriate for the assay of more highly-mixed matrices and how might this be quantified? (iii) How are the optimum performance settings determined for each measurement situation?

Some of the parameters to be determined are the appropriate voxel size (which in turn determines the collimator size and measurement geometry), the measurement dwell time per voxel, and the strength of the transmission source, and the necessary inter-play between the parameters. While a mathematical determination of the optimum parameters may seem reasonable, only an actual performance demonstration serves to convince that the appropriate choice of settings has been implemented for the container size and sample in question.

Canberra has optimized a TGS system to measure 120-liter drums intended primarily for the measurement of plutonium (Pu) bearing waste in a European nuclear fuel reprocessing facility. While this TGS system has the capability to measure containers of various sizes, for the 120-liter container, the system was calibrated and validated with three different spatial resolutions, using two collimator aperture sizes, measuring 2.54 and 1.27 cm in width. (The system has also been calibrated with a wide rectangular collimator for scanning containers solely in the vertical axis; i.e. SGS mode.) The TGS system also has an automated attenuator assembly, with the capability to use a combination of attenuators to reduce the count rate for high activity samples.

In addition to the default standard of  $10 \times 10$  discrete “voxels” per vertical layer for 200L drums, for the 120-liter container, additional scanning protocols of  $14 \times 14$  and  $20 \times 20$  voxel grids were also implemented. Both of the high-resolution modes use the 1.27 cm (1/2 -inch) collimator and a 21-layer scanning protocol to obtain, for the  $14 \times 14$  (“High Resolution” or HR) case, cubic voxels of approximately 3.49 cm per side, and for the  $20 \times 20$  (“Very high resolution” or VHR) case, an elongated rectangular prism shaped voxel of 2.44 cm per side by 3.49 cm high. In the latter case, the elongated voxel shape is a result of legacy data storage limitations of the TGS analysis software. A  $20 \times 20 \times 30$ -layer configuration would have been required to maintain a cubic shape for the VHR configuration, but the resulting 12,000 voxel image could not be processed without substantial modifications to the software. In principle, as long as the voxel grid dimensions are correctly known to the analysis code, the non-cubic shapes are handled without difficulty.

Calibration and verification data are presented in this paper together with a presentation on the importance of capturing the total measurement uncertainty (TMU) associated with the choice of scanning parameters for a given container size.

## **CALIBRATIONS FOR THE HIGH-RESOLUTION CONFIGURATIONS**

For each assay configuration, five calibration assays were performed. In each case, two of the assays used six line sources arranged to simulate a uniform activity distribution in different density matrices, and three used point sources in varied positions in three different density matrices. The calibration measurements were performed using a set of 120 L drums outfitted with manufactured homogenous matrices. The drum standard and matrix combinations used for the calibrations are presented in Table 1.

Matrix	Drum #	Gross Mass (kg)	Matrix Density (g/cc)
Foam	2	16.3	0.03
Soft-board	3	62.6	0.39
MDF	4	94.8	0.68

**Table 1 Calibration Drum Matrix Data**

The calibration drum standards have a series of 9 holes for placement of sources as shown in **Figure 1**. Radial positions 1, 7, and 8 are used with the SGS technique for total measurement uncertainty studies. Positions 2, 3, 4, 5, 6, and 9 have approximately the same radial weights, thereby simulating a uniform distribution of activity when line sources are placed in these positions.

Each line source contains the radioactive isotopes  $^{241}\text{Am}$ ,  $^{133}\text{Ba}$ ,  $^{137}\text{Cs}$  and  $^{60}\text{Co}$ , evenly deposited in an epoxy matrix inside an aluminum casing.

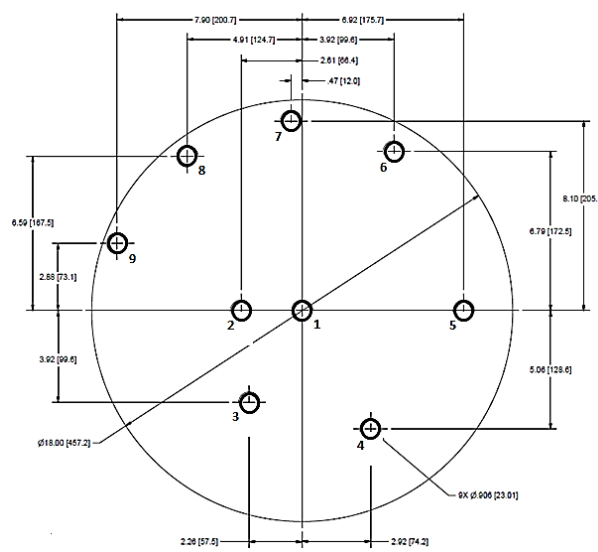


**Figure 1 Drawing of the 120L Calibration Drum Standard Matrix with Source Hole Positions. The dimensions shown are inches [mm].**

The significant emission lines of the calibration nuclides span the range of energies required for quantification of nuclides of interest to the end user. For each gamma ray line of interest in the calibration set, the measured TGS number is combined with source certificate data to calculate the TGS efficiency  $\epsilon$  in units of TGS number per gamma per second (TGS#/gps).

Since the TGS is intended for the assay of nuclides other than those included in the calibration source set, a weighted linear least squares fit is used to interpolate the

TGS efficiency between the measured\_calibration points. The TGS Efficiency can then be combined with nuclear data to obtain Calibration Factors for any line of any desired nuclide. The TGS calibration factor for each gamma ray energy of interest is simply the inverse of the TGS number per unit activity (or per unit mass), such that

$$A = CF \times TGS \# \quad (1)$$

In Equation (1),  $CF$  is the TGS calibration factor in units of either  $\mu\text{Ci} / \text{TGS}\#$  or grams /  $\text{TGS}\#$  of a given nuclide. The assay result  $A$  will be reported according to the units of the calibration factor.

The calibration factors for each energy line of interest in the calibration source could thus be directly determined from the calibration assays, by dividing the measured  $\text{TGS}\#$  for each line by the corresponding nuclide activity. However, users are typically interested in measuring nuclides other than those found in the calibration source. Calibration factors for these lines are mathematically interpolated from the measured calibration data. It is therefore convenient to calculate the TGS efficiency  $\varepsilon$ , in units of  $\text{TGS}\#/\gamma\text{ps}$ , for each line in the calibration source. The TGS efficiency is related to the calibration factor for the  $j^{\text{th}}$  line by

$$CF_j = \frac{1}{\varepsilon(E_j) Y_j 37,000} \quad (2)$$

where  $Y_j$  is the gamma ray yield or intensity and  $E_j$  is the energy of the  $j^{\text{th}}$  line. The factor of  $1/37,000$  converts the result to  $\mu\text{Ci}$ , which are the native units used by the NDA 2000 software.

The efficiency data are fitted as a function of energy by the standard linear least squares method, weighted by the statistical uncertainties of the measured  $\text{TGS}\#$  values, using an empirical function of the form:

$$\text{Log}_{10}(\varepsilon) = AE + B + \frac{C}{E} + \frac{D}{E^2} \quad (3)$$

This is the same form as the "Linear" efficiency function used by Canberra's Genie2000 gamma spectroscopy software.

Once the parameters have been determined, the calibration factors  $CF$  for the lines of other nuclides, beyond those of the calibration set of, may be calculated according to equation (2) using this efficiency function.

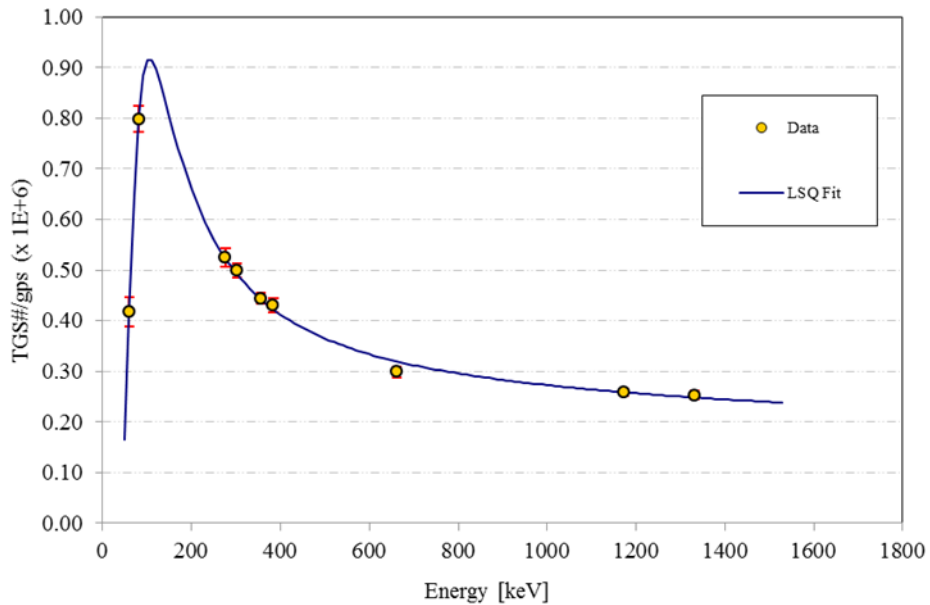


**Figure 2 Example of the fitting of parameterized efficiency curve to the TGS calibration data for the 10x10 resolution**

The calculated calibration factors must be entered into the region of interest (ROI) definition file, along with ROIs for the peak and backgrounds. The measured average TGS efficiency data at each energy of interest, for all three configurations, are presented in Table 2, and plotted for ease of comparison in Figure 3. Not surprisingly, we observe that the TGS efficiency depends on the collimator size; it is nearly identical for the 14x14 and 20x20 resolution configurations, which both use the 1/2" collimator. The 10 x 10 configuration has a higher efficiency at all energies, which is expected given the larger 1" collimator.

Energy (keV)	10x10 TGS Efficiency		14x14 TGS Efficiency		20x20 TGS Efficiency	
	TGS#/yps x10 <sup>6</sup>	Unc.	TGS#/yps x10 <sup>6</sup>	Unc.	TGS#/yps x10 <sup>6</sup>	Unc.
80.998	0.799	0.012	0.329	0.025	0.370	0.017
276.37	0.524	0.008	0.442	0.023	0.132	0.009
302.85	0.499	0.006	0.152	0.009	0.129	0.004
356.01	0.443	0.005	0.141	0.005	0.119	0.003
383.84	0.430	0.006	0.125	0.003	0.108	0.007
661.65	0.298	0.005	0.124	0.008	0.076	0.004
1173.24	0.258	0.004	0.082	0.004	0.088	0.002
1332.51	0.253	0.004	0.071	0.003	0.103	0.003

**Table 2 average TGS efficiency data by energy for standard (10x10), high-resolution (14x14) and very high-resolution (20x20) scanning configurations.**

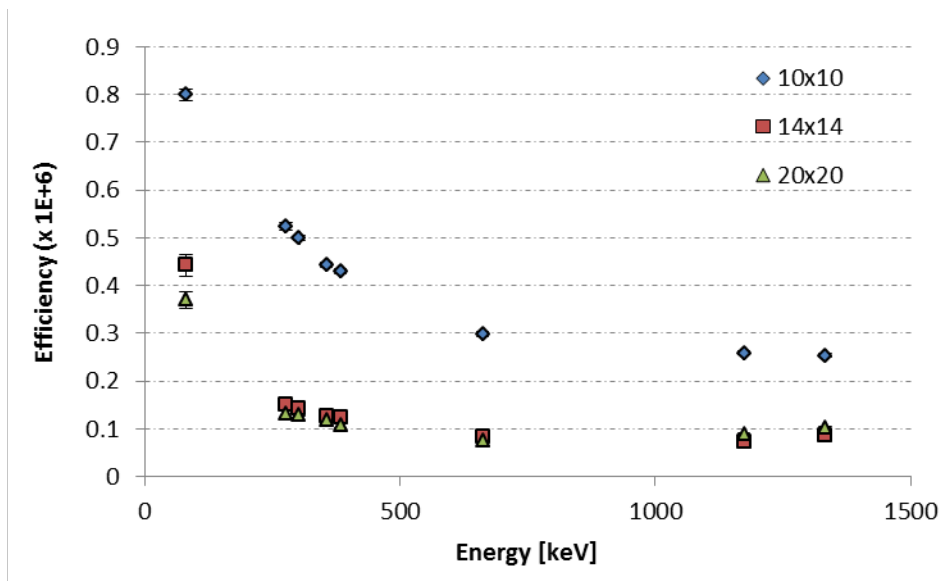


**Figure 3**

## PERFORMANCE EVALUATIONS

The TGS calibration was performed to the mean value of the full set of available measurements, including both line sources and point sources, in matrices of three

different densities. These represent a varied set of source locations and configurations. For an empirical estimate of the TGS assay precision, we can examine the distribution of the individual assays used in the calibration about the mean values.

**10× 10 Standard Resolution**

The distribution of the calibration data about their mean values for the high-resolution scanning configuration is shown in Figure 4. The individual deviations are listed in Table 3, and the RMS average is calculated at each energy. For energies over 100 keV, the RMS variations in the assay results are between 1.2 and 3.2%.

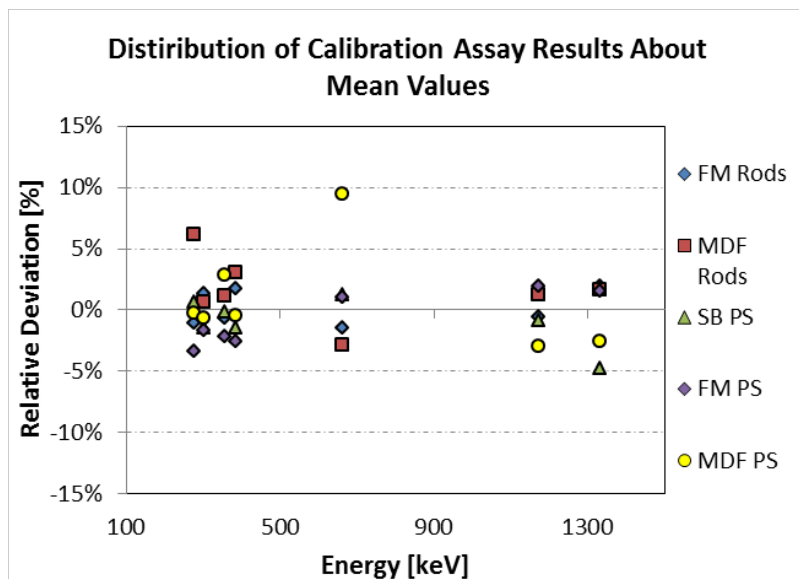


Figure 4 Distributions of calibration results about mean values for the 10×10 resolution.

Energy (keV)	R1	R2	P1	P2	P3	RMS Average
276.37	1.01%	6.2%	0.6%	3.3%	0.3%	3.18%
302.85	1.30%	0.6%	1.5%	1.6%	0.7%	1.21%
356.01	0.60%	1.1%	0.1%	2.2%	2.9%	1.70%
383.84	1.78%	3.0%	1.4%	2.6%	0.5%	2.06%
661.65	1.44%	-2.9%	1.2%	1.0%	9.5%	4.53%

	-	-	-	-	-	-
1173.24	0.56%	1.2%	0.9%	1.9%	3.0%	1.74%
1332.51	1.98%	1.6%	4.8%	1.5%	2.5%	2.76%

**Table 3 Deviations from mean TGS efficiency for individual 10×10 calibration assays for rod (R) and point (P) sources, with calculated RMS average deviations at each energy**

**14×14 High Resolution**

The distribution of calibration data about the mean values for the high-resolution scanning configuration is shown in Figure 4. The individual deviations are listed in [Table 3], and the RMS average is calculated at each energy. For energies over 100 keV, the RMS variations in the assay results are between 5.7 and 16.3%.

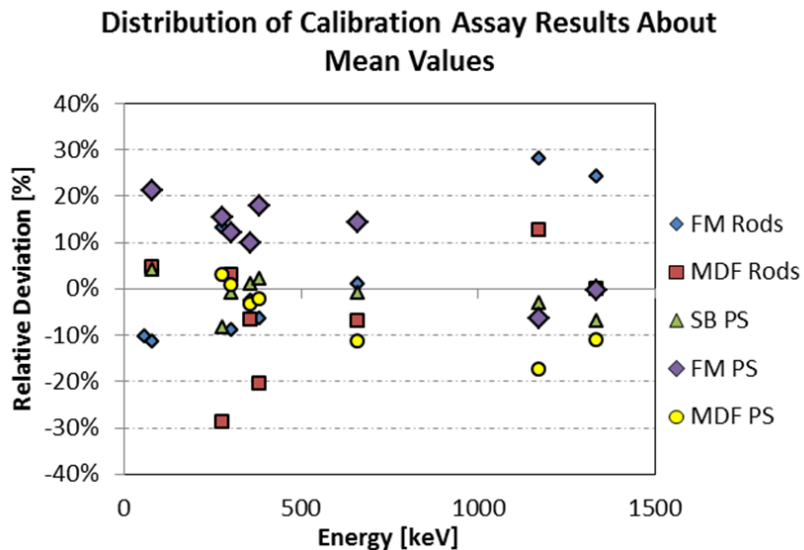


**Figure 5 Distributions of calibration results about mean values for the 14×14 resolution.**

Energy	R1	R2	P1	P2	P3	RMS Avg
-	-	-	-	-	-	-
80.9971	11.23%	4.8%	4.1%	21.1%	41.6%	21.65%
276.37	13.09%	28.7%	8.3%	15.5%	3.1%	16.24%
302.86	-8.76%	3.1%	0.8%	12.1%	0.8%	6.84%



355.99	-2.64%	-6.6%	1.2%	9.9%	-3.5%	5.70%
383.84	-6.36%	20.4%	2.1%	18.0%	-2.1%	12.56%
661.66	1.18%	-6.8%	0.8%	14.2%	11.4%	8.74%
1173.24	28.11%	12.8%	3.1%	-6.4%	17.4%	16.19%
1332.51	24.37%	-0.1%	6.8%	-0.2%	11.1%	12.35%

**Table 4 Deviations from mean TGS efficiency for individual 14x14 calibration assays for rod (R) and point (P) sources, with calculated RMS average deviations at each energy.**

**20x20 Very High Resolution**

The distribution of calibration data about the mean values for the high-resolution scanning configuration is shown in Figure 5. The individual deviations are listed in Table 4, and the RMS average is calculated at each energy. For energies over 100 keV, the RMS variations in the assay results are between 4.7 and 14.3%.

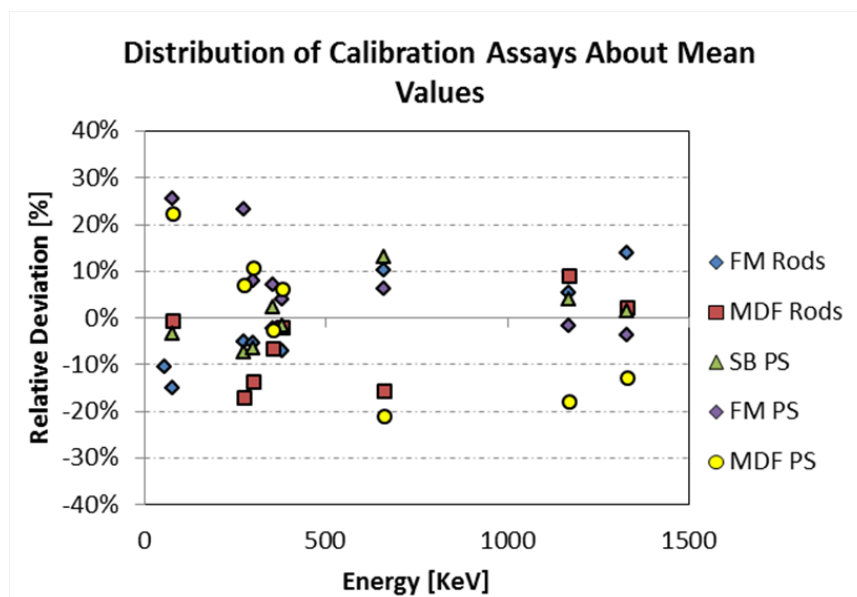


**Figure 6 Distributions of calibration results about mean values for the 20x20 resolution.**

Energy	R1	R2	P1	P2	P3	RMS Avg
80.9971	-	-0.8%	-3.4%	25.5%	22.1%	16.57%

276.37	-5.08%	-	-7.4%	23.3%	6.9%	13.87%
302.86	-5.36%	-	-6.5%	7.8%	10.5%	9.37%
355.99	-2.28%	-6.8%	2.4%	7.0%	-2.8%	4.78%
383.84	-6.94%	-2.3%	-1.7%	4.0%	6.1%	4.68%
661.66	10.36%	-	13.2%	6.4%	-	14.27%
1173.24	5.55%	8.9%	4.1%	-1.7%	-	9.58%
1332.51	13.88%	2.0%	1.4%	-3.7%	-	8.71%

**Table 5 Table 6 Deviations from mean TGS efficiency for individual 20×20 calibration assays for rod (R) and point (P) sources, with calculated RMS average deviations at each energy.**

### ***Comparison to expected results and discussion***

For a “standard” TGS system using a 10×10 voxel scanning resolution we typically expect assay RMS assay to be well within 10%, for single energy lines above 100 keV. This is consistent with the observation of the 10× 10 assay results for this system, where the RMS variability is seen to be less than 5% for all energies. One might naively expect the by simply increasing the scan resolution, a more precise application of voxel-by-voxel attenuation corrections could be achieved, resulting in an overall improvement in assay precision and thus less variability between assays of different source and matrix configurations than we find in the standard configuration. In contrast to that expectation however, we see here a decrease in assay precision for both of the higher resolution (14× 14) scanning configuration, although we note that the performance for the 20× 20 configuration is somewhat improved compared to the 14× 14 configuration.

This is suggestive that the reduced collimator size for the higher resolution scans is in fact the more significant factor in the assay precision, with a smaller collimator resulting in greater assay variability due to perhaps to reduced counting statistics. However, while counting statistics certainly must have some impact on the image reconstruction of the source and matrix distributions, this has been ruled out as the

dominant factor. A number of the calibration assays that showed the highest deviations were replicated immediately, without re-loading the drums or the sources, using longer assay times without significant improvement in the assay results. In these replicate assays, longer individual view times were combined with correspondingly slower drum rotation, such that the volume sampled per view remained unchanged.

The fact that the assay consistency is seen to improve going from the high- to very high-resolution configuration suggests that, other factors being equal, an increased number of voxels of smaller size can indeed improve precision, by allowing for the more accurate application of attenuation corrections and reducing voxel-boundary or so-called "method error" effects .

It is known that there are critical relationships between collimator size and a number of other scanning parameters, including: the source-to-detector distance; the voxel size; the drum diameter; the layer height; the count time; the number of views collected per layer; and the number of drum rotations per scan, among others. The impact of varying each of these parameters in relation to one another in order to create new configurations optimized to assay particular container geometries, differing from the 213 liter or 55-gallon drum for which the TGS methodology was initially developed, is not well understood at the present time. Understanding how to manipulate these relationships to a desired effect is an active area of ongoing research, with opportunities to develop new applications for the TGS technique.

Canberra has previously developed a small scale version of the TGS for the measurement of smaller containers, the so-called "Can-TGS", which performs consistently with the expectations of the full scale standard instrument using the traditional 10× 10 voxel resolution [4]. In that case, the smaller voxel, collimator, source-to-detector distance, etc., are scaled together proportionally and preserve more or less the relationships of the full scale instrument.

## **CONCLUSIONS**

While the TGS system has the capability for scanning at higher resolutions than the default methodology, improved accuracy or performance of the system is not guaranteed simply by choosing a higher resolution. First, an a priori choice of settings does not guarantee improved performance based solely on reducing the voxel size; instead a very careful optimization of the voxel size, collimator size, and dwell time is necessary. Second, even with the optimization, the results are only meaningful in quantification with a very well defined TMU treatment. Third, there are several practical considerations such as longer measurement times, a greater number of default calibrations to be performed, and a greater number and variety of verification measurements needed to validate the optimized settings.

What is recommended as a measurement approach is to first evaluate as best as possible a reasonable trade-off between the sample type (size, content), desired performance, and practical implications of the system setup and calibration. Once this choice has been made it is then essential to implement a TMU protocol. Without it the high-resolution measurements may be impractical in actual usage, and not meaningful in quantification. Lastly, do not discount the applicability of the default settings coupled with a custom post-measurement analysis. This approach is easier to set up in advance, and can be selected for application only when needed, saving time in the pre-measurement instrument setup as well as in the actual measurement itself. Furthermore the TMU in this case may be more mathematically tractable and believable using this approach.

While high-resolution scanning is a capability of the TGS system its applicability must be carefully evaluated case-by-case, and it must be coupled with a very well defined TMU treatment to obtain meaningful quantification results. The usefulness of the capability, however, is as an empirical means to compare and evaluate the value of multiple approaches.

## REFERENCES

1. R. J. Estep, T. H. Prettyman, G. A. Sheppard, *Tomographic gamma scanning to assay heterogeneous radioactive waste*, Nuclear Science and Engineering; Nov. 1994; vol.118, no.3, p.145-52.
2. R. Venkataraman,, M. Villani, S. Croft, P. McClay, R. McElroy, S. Kane, W. Mueller, R. Estep, *An integrated tomographic gamma scanning system for non-destructive assay of radioactive waste*, Nucl. Inst. Meth. in Phys. Res. A 579 (2007), 375-379.
3. S. Croft, D.S. Bracken, S.C. Kane, R. Venkataraman and R. J. Estep, *Bibliography of Tomographic Gamma Scanning Methods Applied to Waste Assay and Nuclear Fuel Measurements*, Proceedings of the 47th Annual Meeting of the INMM (Institute of Nuclear Materials Management), 16-20 July 2006, Nashville, Tennessee, USA.
4. P.J. LeBlanc, J. Lagana, J. Kirkpatrick, D. Nakazawa, S. Kane Smith, R.Venkataraman, M.Villani, and B. M. Young, *Characterization of Canberra's tomographic gamma-ray can scanner ("Can-TGS")*, Proceedings of Waste Management 2013 Conference, February 24 – 28, 2013, Phoenix, Arizona, USA

5. *Standard Test Method for Nondestructive Assay of Radioactive Material by tomographic gamma scanning*, ASTM Standard C1718-10, ASTM International.